A Hybrid Energy Storage System with Reconfigurability and Fast Equalisation

sciendo
Power Electronics and Drives
Volume 7(42), 2022 DOI: 10.2478/pead-2022-0006

A Hybrid Energy Storage System with Reconfigurability and Fast Equalisation

Research paper

Bowen Jiang*, Yujing Liu

Department of Electrical Engineering, Chalmers University of Technology, Gothenburg 41296, Sweden

Received: January 25, 2022; Accepted: March 24, 2022

Abstract: With the rapid growth of electric vehicles (EVs) in recent years, the research on their energy storage systems (ESSs) has also shown great popularity. A traditional ESS normally has a fixed configuration and uses a single type of energy storage unit. However, this traditional design has some limitations, such as low flexibility and high requirements to unit consistency. To solve these problems, a new hybrid energy storage system is proposed in this paper. The proposed ESS hybridises multiple lithium-ion battery modules and one supercapacitor module. By controlling the states of switches inside the ESS topology, module level reconfiguration can be achieved. Further, a DC/DC converter is also included in the ESS topology, which is connected to the supercapacitor module and can be used to ensure correct ESS output voltage. Reconfiguration and active balancing algorithms are also given based on the proposed ESS topology. Situations with and without bypassing the lithium-ion battery modules are both discussed in the algorithms. The proposed hybrid ESS is finally verified with simulations. The system model is built in the Simulink/MATLAB environment. Simulation results show that the lithium-ion modules with a lower state of charge values have higher priorities to be connected in parallel. Reconfiguration actions are able to balance all lithium-ion battery modules within one Worldwide Harmonised Light-Duty Vehicle Test Cycle (WLTC) simulation cycle while maintaining ESS output voltage within a correct range. Furthermore, the proposed hybrid ESS control algorithms remain valid when one lithium-ion battery module is manually bypassed during simulation.

Keywords: *energy storage systems • reconfiguration • active balancing • electric vehicles*

1. Introduction

In recent years, electric vehicles (EVs) have gradually begun to dominate the vehicle market owing to their fewer impacts on the environment, more mature technologies, and continually reducing costs. Energy storage systems (ESSs), as key components in EVs, decide the driving distance, peak acceleration, and many other performance aspects of the vehicles. Lithium-ion batteries are the most common ESSs in EVs. They have many obvious advantages, such as high energy-densities and low self-discharging rates. However, capacity attenuation is a big problem for lithium-ion batteries, which will become even worse after hundreds of cycles. On the other hand, supercapacitors, as another extremely popular ESSs, also attract the attention of many researchers. In contrast with lithium-ion batteries, supercapacitors have much higher power densities owing to their greater charging/discharging currents. Further, the capacity reduction speed is much lower, making them have much longer service lives. However, in comparison with lithium-ion batteries, the energy densities of supercapacitors are smaller and their driving ranges of EVs are also less. Since lithium-ion batteries and supercapacitors show diverse advantages and disadvantages, the idea of mixing the two types of ESSs has been proposed in some previous studies. Following this method, the transient high-power requirements of EVs are stratified with supercapacitors, which is especially valuable during high-acceleration and hard-braking conditions. Meanwhile, lithium-ion batteries can also provide enough energy and maintain long driving distances. Additional electrical circuits are normally needed to build hybrid supercapacitor lithium-ion battery systems. When designing these electrical circuits, many ESS functions can also be developed together: for instance, reconfiguration and active balancing.

* *Email: bowen.jiang@chalmers.se*

Both lithium-ion batteries and supercapacitors are made up of units called modules, which further consist of even smaller units known as cells. Modules and cells are connected in parallel and series to provide the required voltage and current outputs. In a fixed-configuration ESS, the connection configured between these modules and cells cannot be changed during its complete service life. Conversely, a reconfigurable ESS enables different ways of connection. This reconfigurability shows many advantages. First, the total terminal voltage of one ESS can be controlled to different levels and provides power to on-board equipment having different input voltage requirements. Second, if only one or a few units in one ESS have failed, they may be bypassed in a reconfigurable design. This obviates the need for completely scrapping the ESS and can improve the ESS reliability. Third, it is possible to put units with different state of health (SOH) conditions into one ESS, which gives more possibilities for cell recycling. Based on the degree of reconfiguration, there are two levels: cell level and module level. The cell-level reconfiguration ensures individual control of every single cell, which makes it have more flexibility. But at the same time, cell-level reconfiguration requires each cell to be provided a reconfigurable circuit, which would necessitate incurring expenditure on bigger sizes, more costs, and more losses. The module-level reconfiguration only makes the module connections adjustable, while the cell connections inside any one module always remain unchanged. Although the module level reconfiguration has lower flexibility, its control algorithms are much simpler and its reliability is also higher.

The maximum capacities of cells/modules in one ESS are not always exactly the same, which is caused by many reasons, such as manufacturing errors, different degradation speeds, uneven thermal environment, etc. When series-connected units are charged/discharged by the same current, some units will be full/empty earlier than others. If nothing is done to these units, they will be over-charged/over-discharged. This may cause fast-aging, over-heating, or even more serious safety issues. To deal with this problem, the balancing function is conducted by the battery management systems (BMS). Balancing can be categorised into passive balancing and active balancing. The passive balancing uses resistors to dissipate the excessive energy of some units. It is the simplest way of balancing, but also makes the ESS efficiency lower and may bring some thermal problems due to the Joule heat of resistors. On the contrary, active balancing does not need to waste all the exceeding energy and can transfer it among units via some energy storage components. The efficiency of the active balancing is much higher, but it also needs additional circuits and more complex control algorithms.

Based on the above discussion, hybridisation, reconfiguration, and active balancing can all be used to improve ESS performance in different aspects. And a method to integrate the electrical circuits of these three functions would be of great value. Thus, a novel hybrid energy storage system topology is proposed in this paper. The proposed topology connects multiple lithium-ion battery modules and one supercapacitor module together. By changing the states of three switches between every two modules, the EES series/parallel connections can be actively controlled. Further, this system also allows for the failed lithium-ion battery modules to be easily bypassed, thus greatly extending the system lifetime. Additionally, active balancing among lithium-ion battery modules is also achieved using controllable switches. The rest of this paper is arranged as follows: Section 2 introduces the proposed topology and its control methods to realise different connections. Section 3 gives the reconfiguration and active balancing algorithms. Scaled-down Simulink models and simulation results are discussed in section 4, and finally, the conclusions are presented in section 5.

2. Proposed Hybrid Energy Storage System Topology

2.1. Proposed topology components

The proposed hybrid energy storage system topology is shown in Figure 1. Using this topology allows us to achieve module-level hybridisation and reconfiguration. There are totally n lithium-ion battery modules and one supercapacitor module connected together. Between every two neighbouring lithium-ion modules (e.g., M_i and M_{i+1}), there are three switches ($a_{i,1}$, $a_{i,2}$, and $a_{i,3}$).

One DC/DC converter is connected to the supercapacitor module, and they work together to provide an adjustable output voltage. All lithium-ion battery modules together constitute one part, while the DC/DC converter and supercapacitor module constitute the other part. These two parts are also connected by three switches (b_1, b_2, and b_3). Cell connections in modules are always fixed in this topology. And the balancing among cells in any single module can be achieved in a passive way.

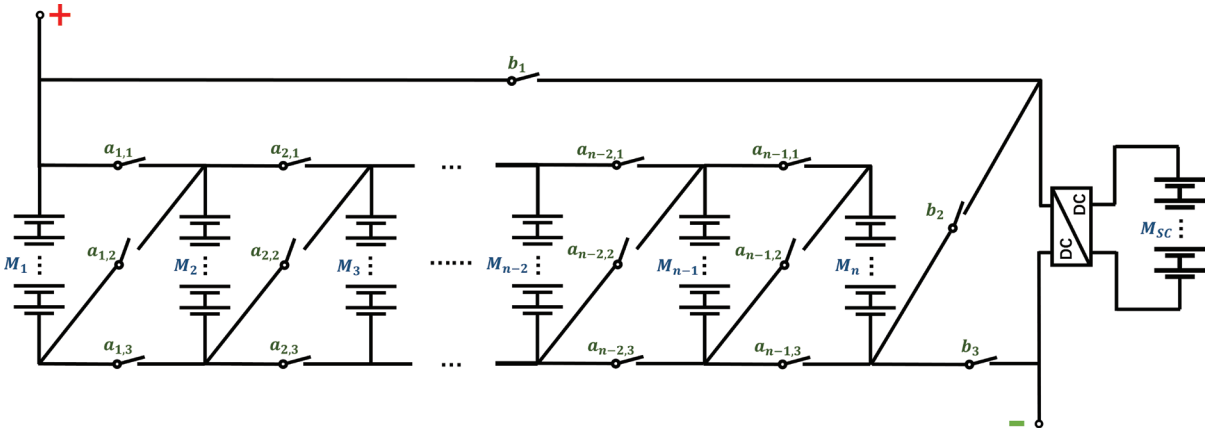

Fig. 1. Proposed hybrid energy storage system topology.

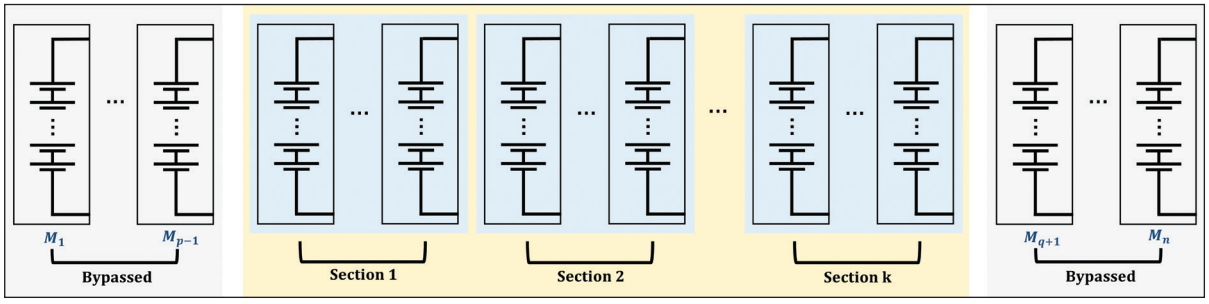

Fig. 2. All lithium-ion battery modules are divided into three parts.

The on-state of a switch is represented by 1, while the off-state of a switch is represented by 0. The information pertaining to all switch states can be summarised in a single matrix:

$$SwitchMatrix = \begin{bmatrix} a_{1,1} & a_{1,2} & a_{1,3} \\ a_{2,1} & a_{2,2} & a_{2,2} \\ \cdots & \cdots & \cdots \\ \cdots & \cdots & \cdots \\ a_{n-2,1} & a_{n-2,2} & a_{n-2,3} \\ a_{n-1,1} & a_{n-1,2} & a_{n-1,3} \\ b_1 & b_2 & b_3 \end{bmatrix} \quad (1)$$

2.2. Proposed topology control

First, the connection control of lithium-ion battery modules is introduced. In order to simplify the control rules of all switches, all lithium-ion battery modules are divided into three parts. As illustrated in Figure 2, the first part starts from the module one and ends before the first battery module, which is not bypassed (named as: M_p). The third part starts after the last connected-in battery module (named as: M_q) and ends with the last battery module. Lastly, the second part is in the middle.

It should be mentioned that it is not necessary to have one/some modules bypassed at the beginning or at the end. The above illustration is just a general case. Also, the rules to control switches in the first and third parts vary, and these rules are listed in Table 1.

The remaining battery modules are divided into multiple sections. Each section contains one or several battery modules. Battery modules in any given section are either connected in parallel (these parallel-connected modules are referred to as a parallel section) or collectively bypassed (these bypassed modules are referred to as a bypass

Table 1. Control rules of switches in the first and third parts.

Modules in the first part	$a_{i,1}=1;\ a_{i,2}=0;\ a_{i,3}=0;\ (i=1,2,\ldots,p-1)$
Modules in the third part	$a_{i,1}=0;\ a_{i,2}=0;\ a_{i,3}=1;\ (i=q,q+1,\ldots,n-1)$

Table 2. Control rules of switches in the second part.

Module M_i is in a parallel section	Module M_{i+1} continues parallel connection	$a_{i,1}=1;\ a_{i,2}=0;\ a_{i,3}=1$
	Module M_{i+1} starts a new parallel section	$a_{i,1}=0;\ a_{i,2}=1;\ a_{i,3}=0$
	Module M_{i+1} starts a new bypass section	$a_{i,1}=0;\ a_{i,2}=0;\ a_{i,3}=1$
Module M_i is in a bypass section	Module M_{i+1} continues bypass connection	$a_{i,1}=0;\ a_{i,2}=0;\ a_{i,3}=1$
	Module M_{i+1} starts a new parallel section	$a_{i,1}=0;\ a_{i,2}=1;\ a_{i,3}=0$

Table 3. Control rules of switches before the supercapacitor module.

Supercapacitor module M_{sc} is connected in parallel with lithium-ion battery modules	$b_1=1;\ b_2=0;\ b_3=1$
Supercapacitor module M_{sc} is connected in series with lithium-ion battery modules	$b_1=0;\ b_2=1;\ b_3=0$
Supercapacitor module M_{sc} is bypassed	$b_1=0;\ b_2=0;\ b_3=1$

section). All sections are in series connection. The rules of controlling switches in the second part are shown in Table 2.

The proposed topology still has some limitations in realising all modes of connections. For example, it is not possible to have two non-adjacent battery modules in a parallel connection. Also, one battery module cannot be parallelly connected to two ends of multiple battery modules that are already in series connection. These modes will be possible if more switches are added, but it will also make the system more complex and result in increased costs.

The supercapacitor module and the DC/DC converter are combined, and then connected to the circuit. Similarly, the supercapacitor module and all lithium-ion battery modules can be in either series or parallel connection. Further, it is also possible to directly bypass the supercapacitor module. The rules of controlling the three switches before the supercapacitor module are described in Table 3.

3. Reconfiguration and Active Balancing Algorithms

The reconfiguration algorithms introduced in this section aim to achieve fast active balancing. Two cases are considered here. One is without bypassing any lithium-ion battery module, and the other is with bypassing only one lithium-ion battery module. The possibility of having two or more battery modules fail earlier than the other battery modules is very low. When this happens, the ESS normally needs to be maintained. So, the case of having more than one battery module bypassed is not considered in the following algorithms.

3.1. Active balancing without bypassing module

In an electric powertrain system, the ESS provides power to the inverter, which drives the electric machine, giving output torque. The inverter and electric machine require the EES output voltage to be maintained within a certain range. An average voltage can be calculated from this range. This is the required voltage ($V_{require}$), which should be provided by the ESS. Terminal voltage values of all lithium-ion battery modules are measured, whose average is calculated as $\overline{V_{module}}$. When no battery module is bypassed, the number of required battery module sections (m) can be determined according to the following equation:

$$m\cdot\overline{V_{module}}<V_{require}<(m+1)\cdot\overline{V_{module}} \tag{2}$$

Afterwards, all battery modules need to be sliced into m sections. An example is given below when there are six battery modules. All possible options for a given section number are listed. The battery modules in the same section have the same background colour.

6 modules, 6 sections: 1 option

Module 1	Module 2	Module 3	Module 4	Module 5	Module 6

6 modules, 5 sections: 5 options

Module 1	Module 2	Module 3	Module 4	Module 5	Module 6
Module 1	Module 2	Module 3	Module 4	Module 5	Module 6
Module 1	Module 2	Module 3	Module 4	Module 5	Module 6
Module 1	Module 2	Module 3	Module 4	Module 5	Module 6
Module 1	Module 2	Module 3	Module 4	Module 5	Module 6

6 modules, 4 sections: 10 options

Module 1	Module 2	Module 3	Module 4	Module 5	Module 6
Module 1	Module 2	Module 3	Module 4	Module 5	Module 6
Module 1	Module 2	Module 3	Module 4	Module 5	Module 6
Module 1	Module 2	Module 3	Module 4	Module 5	Module 6
Module 1	Module 2	Module 3	Module 4	Module 5	Module 6
Module 1	Module 2	Module 3	Module 4	Module 5	Module 6
Module 1	Module 2	Module 3	Module 4	Module 5	Module 6
Module 1	Module 2	Module 3	Module 4	Module 5	Module 6
Module 1	Module 2	Module 3	Module 4	Module 5	Module 6
Module 1	Module 2	Module 3	Module 4	Module 5	Module 6

6 modules, 3 sections: 10 options

Module 1	Module 2	Module 3	Module 4	Module 5	Module 6
Module 1	Module 2	Module 3	Module 4	Module 5	Module 6
Module 1	Module 2	Module 3	Module 4	Module 5	Module 6
Module 1	Module 2	Module 3	Module 4	Module 5	Module 6
Module 1	Module 2	Module 3	Module 4	Module 5	Module 6
Module 1	Module 2	Module 3	Module 4	Module 5	Module 6
Module 1	Module 2	Module 3	Module 4	Module 5	Module 6
Module 1	Module 2	Module 3	Module 4	Module 5	Module 6
Module 1	Module 2	Module 3	Module 4	Module 5	Module 6
Module 1	Module 2	Module 3	Module 4	Module 5	Module 6

6 modules, 2 sections: 5 options

Module 1	Module 2	Module 3	Module 4	Module 5	Module 6
Module 1	Module 2	Module 3	Module 4	Module 5	Module 6
Module 1	Module 2	Module 3	Module 4	Module 5	Module 6
Module 1	Module 2	Module 3	Module 4	Module 5	Module 6
Module 1	Module 2	Module 3	Module 4	Module 5	Module 6

6 modules, 1 section: 1 option

Module 1	Module 2	Module 3	Module 4	Module 5	Module 6

When battery module number in the ESS is increased to and the section number is m, all possible solutions can be found according to the following algorithms:

Algorithms: Find all options for a given battery module number and a section number

Inputs: n: module number, m: section number
Output: S.: set of all possible options
Global: s.: one possible option

for $i_1 = 1:1:(m - n + 1)$.

$s(1) = i_1;$

for $i_2 = 1:1:((m - i_1) - (n - 1) + 1)$

$s(2) = i_2;$

for $i_3 = 1:1:((m - i_1 - i_2) - (n - 2) + 1)$

$s(3) = i_3;$

… … … … … …
… … … … … …

for $i_m = 1:1:((m - i_1 - i_2 ...... - i_{m-1}) - (n - m + 1) + 1)$

$s(m) = i_m;$

```
                    if s ∉ S
                        S = [S;s];
                    end
                end
            … … … … … …
            … … … … … …
        end
    end
end
```

After all possible options are found for a given section number (m), the next step is to select the best option that can achieve the fastest active balancing. The state of charge (SOC) and estimated capacity information of all battery modules can be obtained from the BMS. The average SOC value of all battery modules is calculated as $\overline{\mathrm{SOC}}$, which is used to create a $1 \times m$ vector, as shown below:

$$\overrightarrow{\overline{SOC}_0} = \left(\overline{SOC},\ \overline{SOC},\ \overline{SOC},\ldots,\ \overline{SOC}\right) \tag{3}$$

For each possible option (e.g., option i), the average SOC value of each section can be calculated. Another $1 \times m$ vector is created, as shown below:

$$\overrightarrow{\overline{SOC}_{i,\ be}} = \left(\overline{SOC_{be,sec1}},\ \overline{SOC_{be,sec2}},\ \overline{SOC_{be,sec3}},\ldots,\ \overline{SOC_{be,secm}}\right) \tag{4}$$

Similarly, two more vectors can additionally be created based on the average capacity values and battery module numbers of all the sections:

$$\overrightarrow{\overline{Q}_i} = \left(\overline{Q_{sec1}},\ \overline{Q_{sec2}},\ \overline{Q_{sec3}},\ldots,\ \overline{Q_{secm}}\right) \tag{5}$$

$$\overrightarrow{\overline{N}_i} = \left(N_{sec1},\ N_{sec2},\ N_{sec3},\ldots,\ N_{secm}\right) \tag{6}$$

The discharging current in the ESS main circuit (I_d) can also be obtained from the BMS. After the ESS is discharged for a certain period t_1, the average SOC value of battery modules in the section j is calculated as indicated below:

$$\overline{SOC_{af,secj}} = \overline{SOC_{be,secj}} - \frac{I_d \cdot t_1}{\overline{Q_{secj}} \cdot N_{secj}} \tag{7}$$

Similarly, using the vector indicated below, it becomes possible to compute the average SOC values of all sections after a certain period of discharging:

$$\overrightarrow{\overline{SOC}_{i,\ af}} = \left(\overline{SOC_{af,sec1}},\ \overline{SOC_{af,sec2}},\ \overline{SOC_{af,sec3}},\ldots,\ \overline{SOC_{af,secm}}\right) \tag{8}$$

Finally, the best option can be selected based on the following criteria:

$$min\left(\left|\overrightarrow{\overline{SOC}_0} - \overrightarrow{\overline{SOC}_{i,\ af}}\right|\right) \tag{9}$$

In this proposed active balancing method, the supercapacitor model is always in series connection with the other lithium-ion battery modules. However, the voltage conversion ratio of the DC/DC converter is adjustable. After the best option of lithium-ion battery module connection is selected, the next step is to select the correct voltage conversion ratio. As discussed earlier, to enable the effective operation of the inverter and electric machine, the output voltage of the ESS needs to be maintained within a certain range. The upper and lower voltage limits of the ESS are defined as V_{high} and V_{low}, respectively. The terminal voltage of the section j, named $\overline{V_{secj}}$, can also be calculated from the battery module voltages. The output voltage of the DC/DC converter ($V_{converter}$) can thus be calculated according to the following equation:

$$V_{low} - \sum_{j=1}^{m} \overline{V_{secj}} < V_{converter} < V_{high} - \sum_{j=1}^{m} \overline{V_{secj}} \ . \tag{10}$$

The boost/buck voltage conversion ratio of the DC/DC converter can finally be calculated according to the following equation:

$$R_{converter} = \frac{V_{converter}}{V_{SC}} \tag{11}$$

where V_{SC} is the terminal voltage of the supercapacitor module. To achieve continuous active balancing, the above process shall be repeated for every certain period of t_1. The suitable section number, best option of battery connection, and suitable DC/DC converter voltage conversion ratio shall also be updated.

3.2. Active balancing with bypassing one module

There are two different situations when one lithium-ion battery module is bypassed. The first situation is when the bypassed battery module is either in the beginning or at the end. The problem of dividing n battery modules into m sections can be transformed into one of dividing $n-1$ battery modules into m sections. Under this situation, the same algorithms as before can be used to find all possible battery connection options. One example is given below, when there are six battery modules and the first one is bypassed.

6 modules, 5 sections, the first module is bypassed: 1 option

6 modules, 4 sections, the first module is bypassed: 4 options

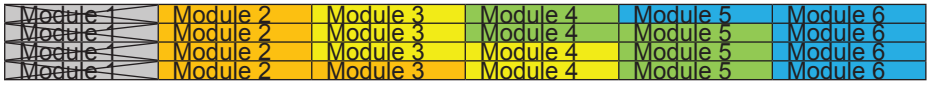

6 modules, 3 sections, the first module is bypassed: 6 options

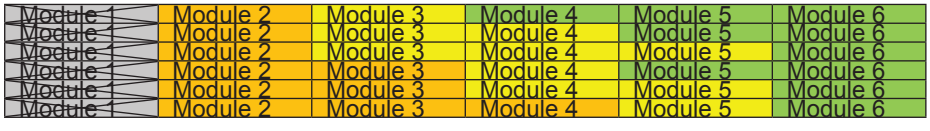

6 modules, 2 sections, the first module is bypassed: 4 options

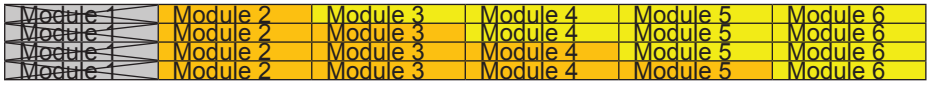

6 modules, 1 sections, the first module is bypassed: 1 option

The second situation is when the bypassed battery module is in the middle. The number of battery modules before and after the bypassed one are defined as r_1 and r_2, respectively. The problem of dividing n modules into m

sections can be transformed into one of dividing r_1 modules into w_1 sections and dividing r_2 modules into w_2 sections. r_1, r_2, w_1, and w_2 shall meet the following restrictions:

$$\begin{cases} r_1 + r_2 = n - 1 \\ w_1 + w_2 = m \\ r_1 \geq w_1 \\ r_2 \geq w_2 \end{cases} \tag{12}$$

One example is given below, when there are six battery modules and the third one is bypassed.

6 modules, 5 sections, the third module failed: 1 option

6 modules, 4 sections, the third module failed: 3 options

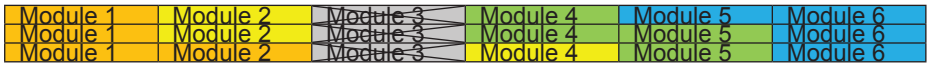

6 modules, 3 sections, the third module failed: 3 options

6 modules, 2 sections, the third module failed: 1 option

The algorithms introduced in section 3.1 are integrated as a function and named 'selection'. The following algorithms are used to find all possible options when there is a bypassed module in the middle.

Algorithms: Find all options when a middle module is bypassed

Inputs: n: module number, m: section number
r_1: module number before the bypassed module
r_2: module number after the bypassed module
Output: S: set of all possible options
Global: s: one possible option

```
for i = 1:1:r1
    If r2 < m - i || m - i ≤ 0
        stop;
    end
    S1 = selection(r1, i);
    S2 = selection(r2, m - i);
    for j = 1:1:size(S1,1)
        for k = 1:1:size(S2,1)
            s = [S1(j,:), S2(k,:)]
            S = [S, s]
        end
    end
end
```

4. Simulink Modelling and Simulation Results

4.1. Simulink modelling

Modelling and simulation have been done to verify the proposed hybrid ESS topology and control algorithms. A scaled-down hybrid ESS is built in the Simulink environment, which consists of eight lithium-ion cells, one supercapacitor cell, and one DC/DC converter. Some parameters of the built ESS module are listed in Table 4.

Table 4. Hybrid ESS model parameters.

Hybrid ESS Model Parameters	Variable	Value	Unit
Lithium-ion cell capacity	C_{li}	24	Ah
Lithium-ion cell nominal voltage	$V_{li,nom}$	3.7	V
Lithium-ion cell lower voltage limit	$V_{li,low}$	2.5	V
Lithium-ion cell upper voltage limit	$V_{li,high}$	4.2	V
Lithium-ion cell number	n_{li}	8	–
Supercapacitor cell capacity	C_{SC}	3,000	F
Supercapacitor cell lower voltage limit	$V_{SC,low}$	0.5	V
Supercapacitor cell upper voltage limit	$V_{SC,high}$	2.8	V
ESS lower voltage limit	$V_{ESS,low}$	29	V
ESS upper voltage limit	$V_{ESS,high}$	33	V

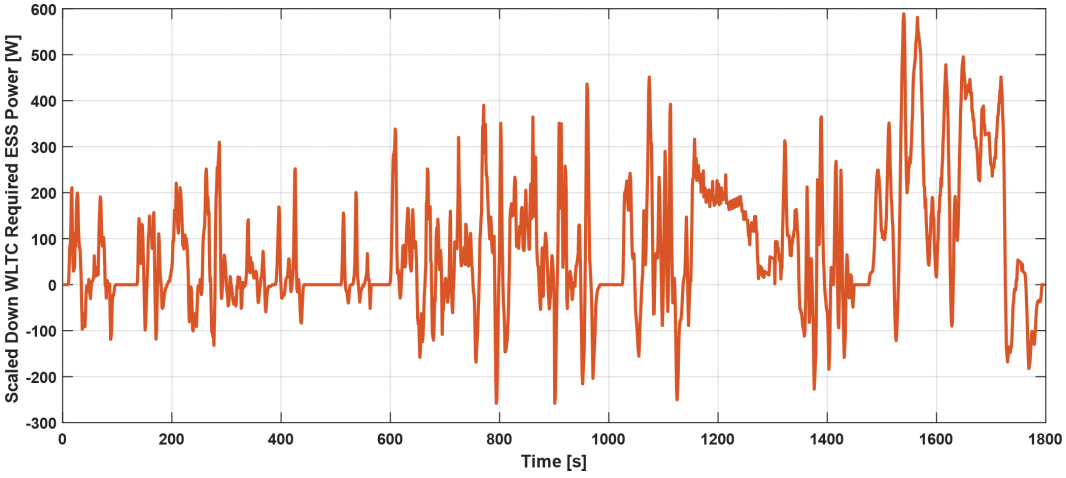

Fig. 3. Scaled-down WLTC required ESS power. ESS, energy storage system; WLTC, Worldwide Harmonised Light-Duty Vehicle Test Cycle.

In selecting the DC/DC converter, it is necessary to consider the cell and ESS parameters. The input voltage range of the DC/DC converter shall be the same as the supercapacitor cell output voltage range: $\left[V_{SC,low},\ V_{SC,high}\right]$.

The output voltage range of the DC/DC converter can be calculated with the output voltage ranges of one lithium-ion cell and the complete ESS: $\left[V_{ESS,high} - n_{li} \cdot V_{li,high},\ V_{ESS,low} - V_{li,low}\right]$. The maximum input and output currents of the DC/DC converter shall be smaller than the maximum supercapacitor cell discharging current and the maximum lithium-ion cell discharging current, respectively.

The hybrid ESS model is assumed to be used in medium-size electric vehicles (e.g., Tesla Model S), and 'Worldwide Harmonised Light-Duty Vehicle Test Cycle (WLTC)' is selected to be the simulation driving cycle. The reference vehicle parameters and driving cycle data are used to calculate the required power to the hybrid ESS (the detailed calculation process is not covered in this paper). Based on the capacity difference between the reference vehicle ESS and the modelled hybrid ESS, the calculated power is also scaled down, and plotted in Figure 3. The positive values mean that the ESS needs to provide the power to drive the vehicle, while the negative values mean that the vehicle is braked and regenerated power is sent back to the ESS.

Each lithium-ion cell is modelled with a two-resistor-capacitor (two-RC) equivalent circuit, as shown in Figure 4. R_0 represents the Ohmic resistance of the current collectors, electrolyte, separator, etc. The first RC couple (R_1–C_1) represents the charge transfer process happening inside the electrode active material. The second RC couple (R_2–C_2) represents the lithium-ion diffusion process happening inside and outside the active material particles. Only irreversible heat (Joule heat) is considered inside the lithium-ion cell model. A simplified cooling system is modelled, which consists of coolant heat convection and heat conduction. The simulated cell temperature and SOC are used to determine the values of R_0, R_1, C_1, R_2, and C_2 using several look-up tables. The parameters of the lithium-ion cell equivalent circuit are continuously and actively adjusted during the simulation. Coulomb counting

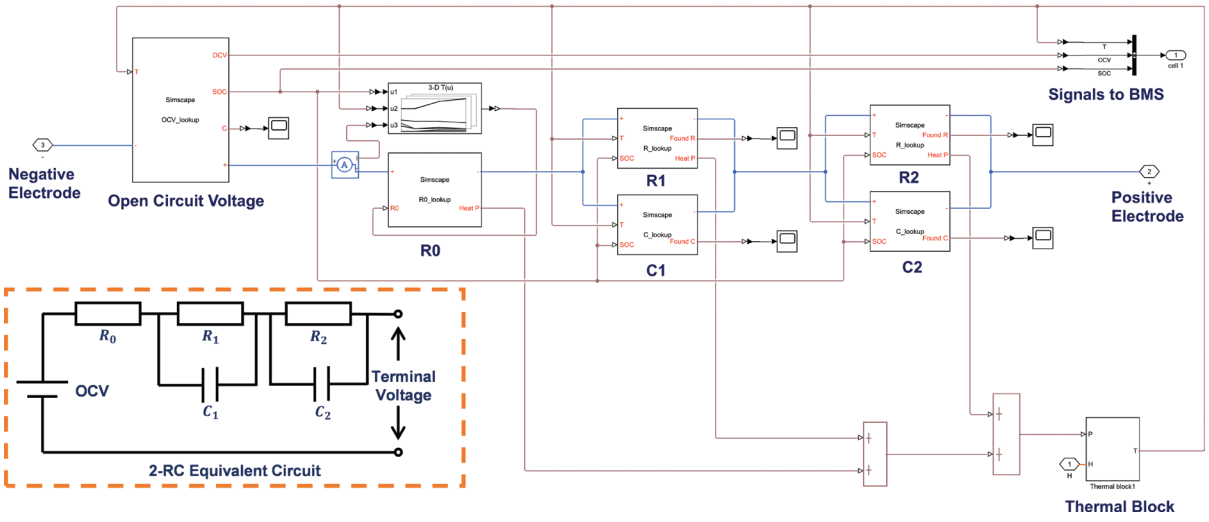

Fig. 4. Equivalent circuit model of one lithium-ion cell.

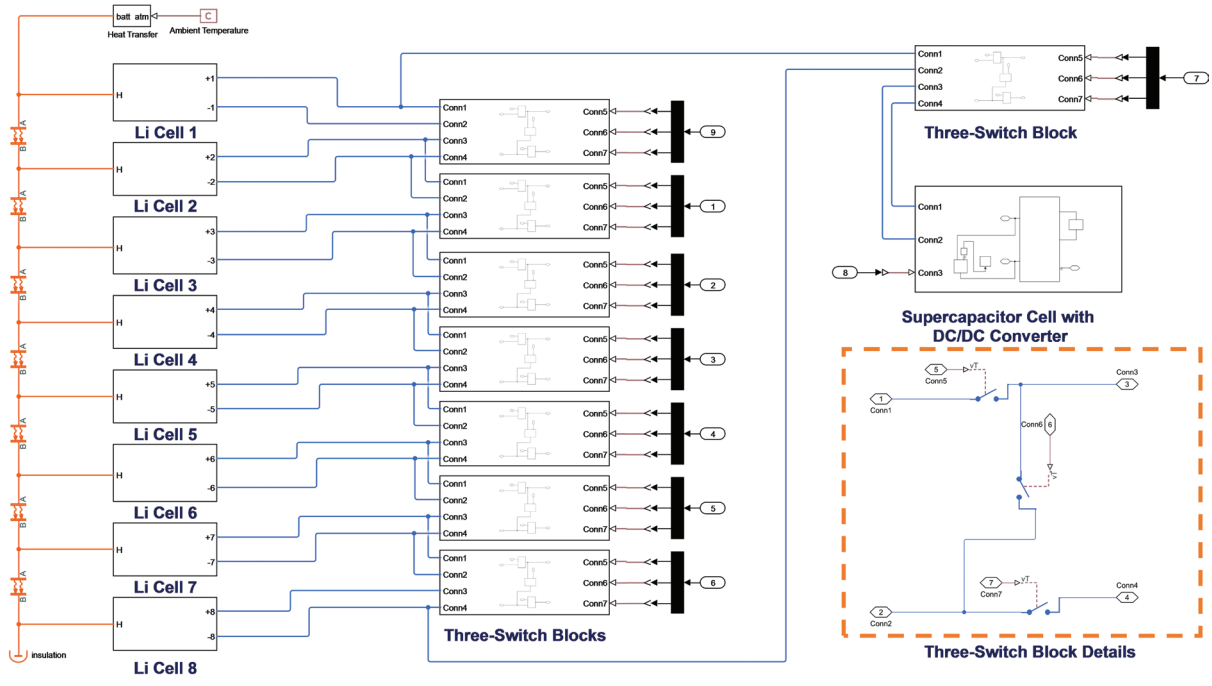

Fig. 5. Complete model of the hybrid ESS. ESS, energy storage systems.

is the SOC estimation method used in the lithium-ion cell model. The signals of SOC, open circuit voltage (OCV), and temperature are continuously sent to the BMS of the hybrid ESS.

The complete hybrid ESS model is shown in Figure 5. The lithium-ion cell equivalent circuit model is integrated into one block, and there are totally eight lithium-ion cell blocks. The supercapacitor cell and DC/DC converter are modelled directly using units from the Simulink package provided by MATLAB/Simulink, and they are put together into one block. Three switches between two battery modules are integrated into one block. There are totally eight three-switch blocks connecting eight lithium-ion cells and one supercapacitor cell together, according to the layout shown in Figure 1. Finally, the switch control signals and the DC/DC converter voltage conversion ratio signal are

sent from BMS. The BMS is modelled as a MATLAB function, which is not included in Figure 5. The reconfiguration and active balancing algorithms introduced in section 3 are all coded in the BMS function.

4.2. Simulation results

Two cases have been simulated with the hybrid ESS model and the WLTC driving cycle. The first case has no lithium-ion cell bypassed. SOC curves of the eight lithium-ion cells are plotted in Figure 6, which presents the active balancing performance. In Figure 7, charging/discharging currents of lithium-ion cells 1, 3, and 5 are plotted with red, blue, and green curves, respectively. In order to observe the active balancing performance, the initial SOC values of the eight lithium-ion cells are set differently. Lithium-ion cell 1 has the smallest initial SOC, followed by cells 2, 6, 7, and 5. The other three lithium-ion cells are all fully charged at the beginning. As mentioned earlier, the first step of the active balancing algorithms is to decide how many series-connected sections are needed. This calculation is based on the required ESS voltage and the average voltage of all lithium-ion cells. In the first case simulation, this number is 7V. This means two lithium-ion cells needed to be parallelly connected, and they are together in series connection with the other six lithium-ion cells as well as the supercapacitor cell. By selecting two different parallelly connected

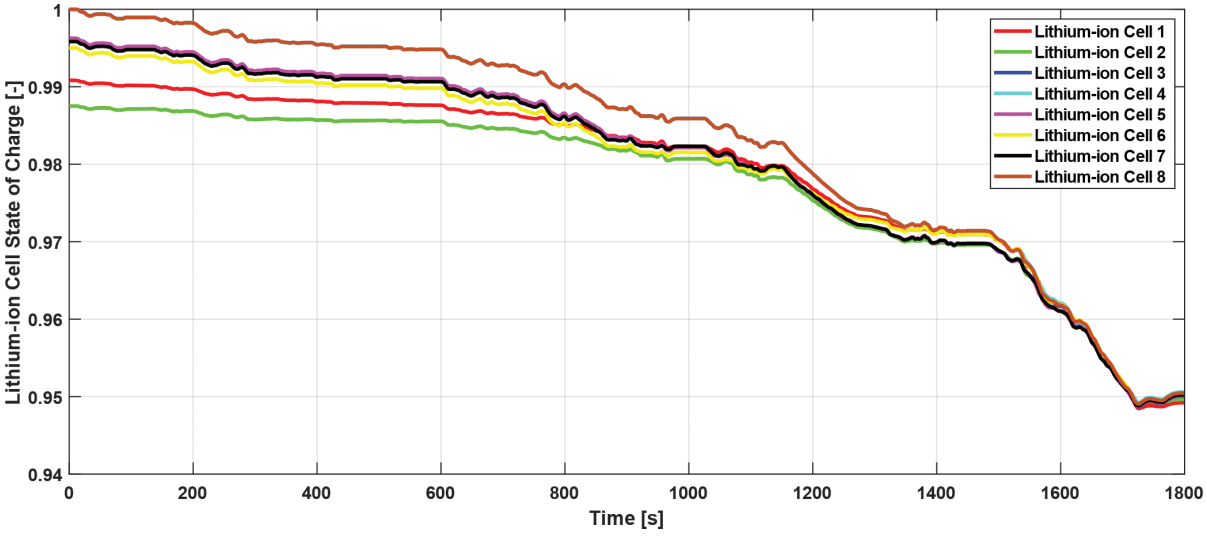

Fig. 6. State of charge balancing curves of eight lithium-ion cells (with no bypassed cell).

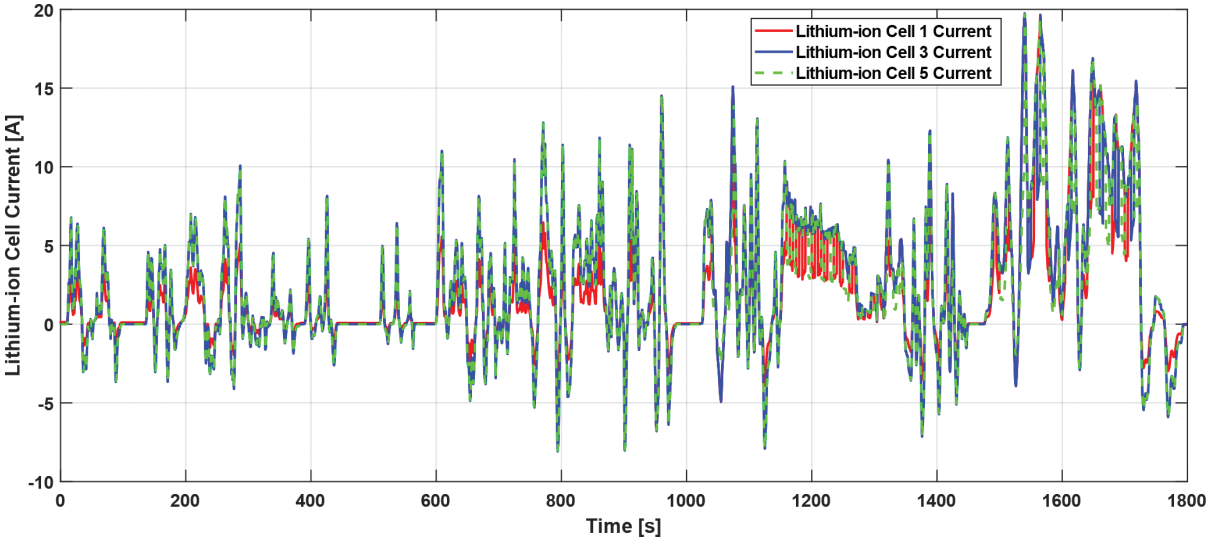

Fig. 7. Current curves of lithium-ion cells 1, 3, and 5 (with no bypassed cell).

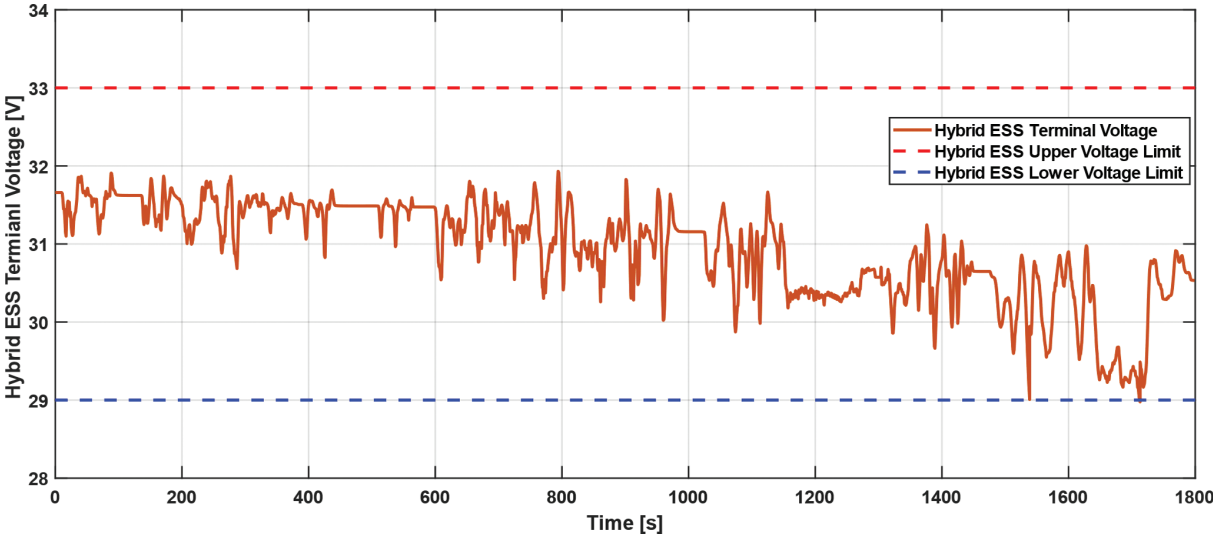

Fig. 8. Hybrid ESS terminal voltage (with no bypassed cell). ESS, energy storage system.

lithium-ion cells, the SOC of the eight lithium-ion cells can be balanced. Due to the limitation of the proposed topology, only neighbouring lithium-ion cells can be connected in parallel. From Figure 6, it can be observed that, in the beginning, the SOC of lithium-ion cells 1 and 2 are the two smallest values. As a result, they are connected in parallel according to the active balancing algorithms, and their SOC decreasing speeds are also smaller than those of the other six lithium-ion cells in the beginning. The same result can be observed in Figure 7. During the first 870 s, the current of lithium-ion cell 1 is only half of those of cells 3 and 5. This is also due to the parallel connection of lithium-ion cells 1 and 2, resulting in their consuming only half as much energy compared to the other six cells.

After the point of 870 s, the SOC value sum of lithium-ion cells 6 and 7 becomes smaller than those for the other neighbouring cell couples. So, the reconfiguration is conducted at this moment, and the parallel connection is changed to lithium-ion cells 6 and 7. In Figure 7, it can be observed that during the 20 s after the occurrence of the first reconfiguration, currents of lithium-ion cells 1, 3, and 5 were all the same. This is because these three cells were all connected in series at that moment. Afterwards, reconfiguration actions keep happening. Parallel-connected cell couples are also continuously changing among cells 1 and 2, 5 and 6, and 6 and 7. The complete balancing of eight lithium-ion cells is achieved at 1,645 s, when parallel connection occurs evenly among them. It should be mentioned that the best configuration is calculated once per interval (a duration of 5 s is used here). This means that one configuration is kept for at least 5 s. This can avoid excessive calculation load on BMS, as well as excessive switching losses.

The terminal voltage of the complete hybrid ESS is plotted in Figure 8. It can be observed that the ESS terminal voltage is always kept between 29 V (blue dash line) and 33 V (red dash line). They are the ESS lower and upper voltage limits, respectively. As mentioned earlier, the optimal voltage conversion ratio of the DC/DC converter is updated at every calculation interval. This ensures that the hybrid ESS terminal voltage will always be within the correct range.

The second case is to have one lithium-ion cell bypassed during the driving cycle simulation. The lithium-ion cell SOC curves and current curves of the second case are shown in Figures 9 and 10, respectively. Compared to the first case, the balancing process of the first 1,000 s is kept unchanged due to the same initial settings. At the point of 1,000 s, lithium-ion cell 5 is manually bypassed. From Figure 9, it can be observed that the SOC value of lithium-ion cell 5 is kept unchanged after it is bypassed. At the same time, as can be seen in Figure 10, the lithium-ion cell 5 current also decreases to 0V. After one lithium-ion cell is bypassed, the proposed reconfiguration algorithms continue to calculate the optimal connection. As can be observed from Figure 10, the seven other lithium-ion cells continue to be balanced after the point of 1,000 s. Similar to the first case, two lithium-ion cell couples (cells 1 and 2 and cells 6 and 7) are alternatively connected in parallel. Finally, at the point of 1,725 s, all seven in-use lithium-ion cells are balanced.

The hybrid ESS terminal voltage of the second case simulation, together with the ESS lower and upper voltage limits, is shown in Figure 11. Compared to the first case, the voltage touching the lower limit comes earlier. This is

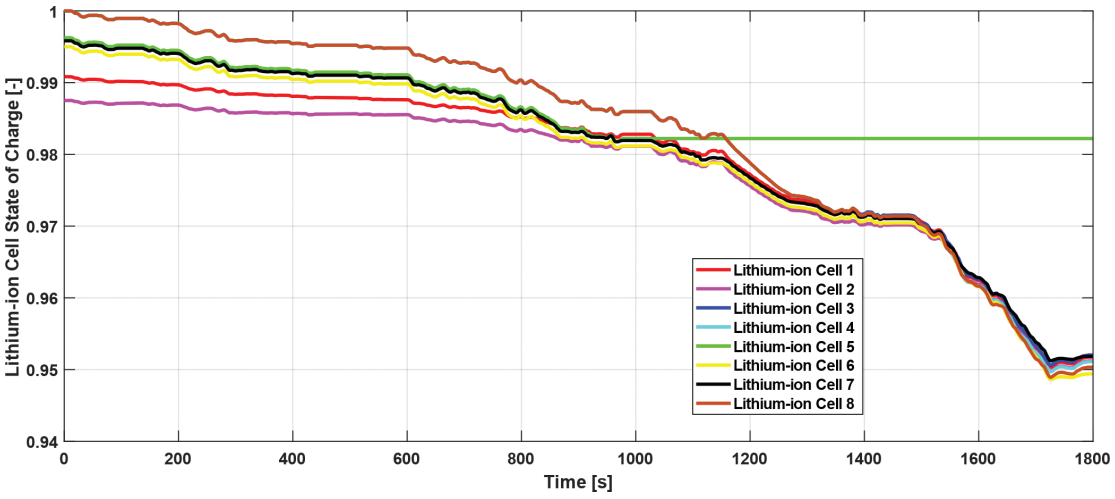

Fig. 9. State of charge balancing curves of eight lithium-ion cells (with the lithium-ion cell 5 bypassed).

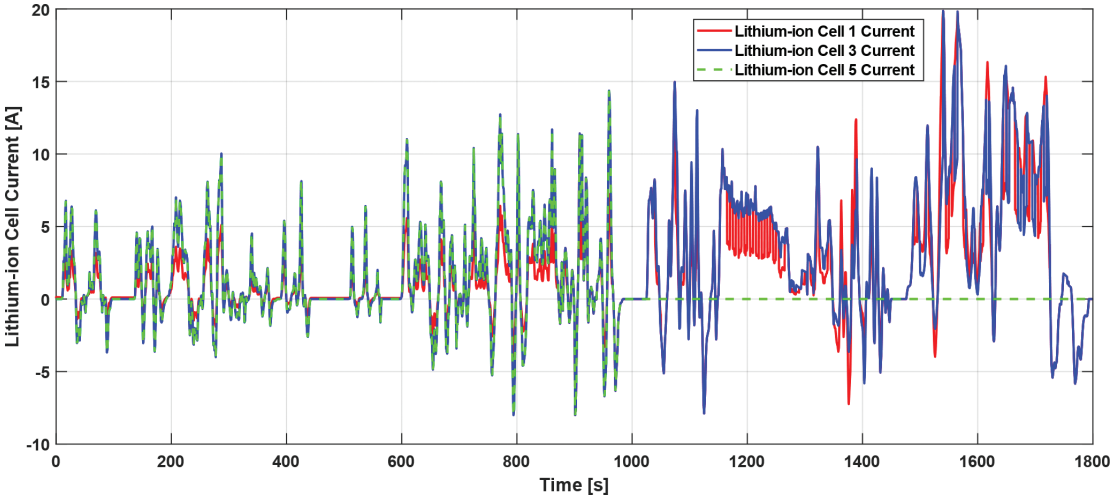

Fig. 10. Current curves of lithium-ion cells 1, 3, and 5 (with lithium-ion cell 5 bypassed).

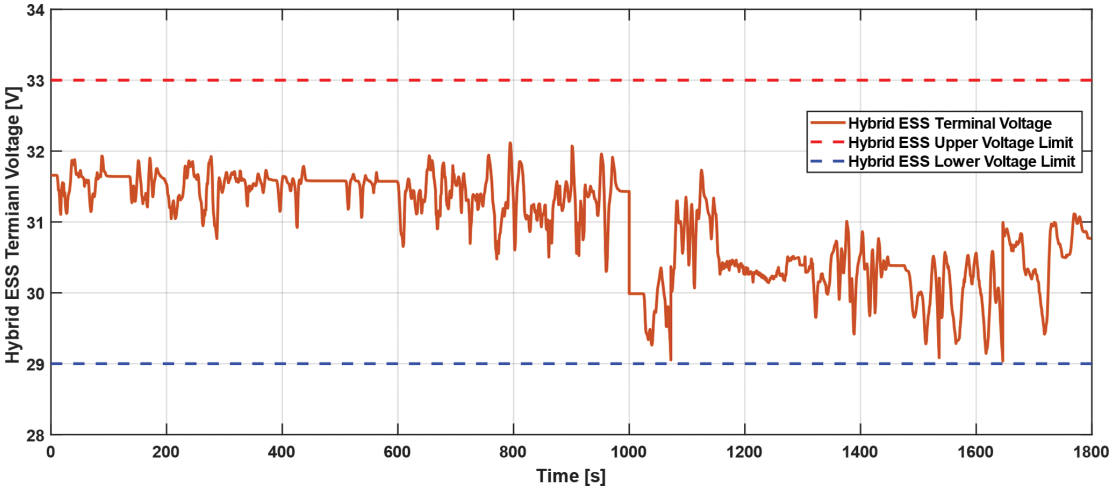

Fig. 11. Hybrid ESS terminal voltage (with lithium-ion cell 5 bypassed). ESS, energy storage system.

because fewer lithium-ion cells need to provide the same required power, making the hybrid ESS terminal voltage decrease faster. However, the hybrid ESS terminal voltage is still maintained above the lower limit by correctly controlling the voltage conversion ratio of the DC/DC converter.

5. Conclusions

In this paper, a new topology of a hybrid ESS is proposed, which consists of multiple lithium-ion battery modules, one supercapacitor module, one DC/DC converter, and some switches. The proposed topology has highly flexible module-level reconfiguration. By controlling switch states, parallel, series, and bypass connections can all be achieved. Detailed algorithms to find out all possible configurations and to conduct fast active balancing are given. Situations with and without the lithium-ion battery modules being bypassed are both discussed. Further, by correctly controlling the voltage conversion ratio of the DC/DC converter, the terminal voltage of the complete hybrid ESS can be maintained. The proposed topology and algorithms are finally verified with Simulink modelling and simulation. A scaled-down hybrid ESS model is built, which utilises a two-RC equivalent circuit to model the lithium-ion cells, and the Simscape package to model the supercapacitor cell. Two cases are simulated. The first case has no cell bypassed, while the second case has the lithium-ion cell 5 bypassed. Since this proposed hybrid ESS is mainly designed for vehicle applications, the required power is calculated from the WLTC driving cycle in both cases. Simulation results show that lithium-ion cells with lower SOC values have higher priorities to be connected in parallel, which makes them have smaller discharging currents and consume less energy compared with other lithium-ion cells. A fully balanced state can be finally achieved within one driving cycle. The proposed algorithms are effective when one lithium-cell is bypassed in the middle of the driving cycle simulation. Further, during the reconfiguration active balancing processes in both simulated cases, the terminal voltage of the hybrid ESS is successfully controlled within the correct range.

However, there are still some limitations characterising the proposed hybrid ESS topology and active balancing algorithms. First, insulated-gate bipolar transistor (IGBT) or metal oxide semiconductor field effect transistor (MOSFET) devices can be selected as switches in the proposed ESS topology. When the ESS is operated under a certain configuration, conduction losses may exist with switches that are in the on-state. When reconfiguration actions happen, switching losses may exist with switches whose states are changed. Although the switches are not operated at high frequencies according to the proposed active balancing algorithms, the sum of conduction and switching losses can still reduce the ESS efficiency to some extent. Second, after the ESS has been used for a long time, the ageing of the switches can affect ESS performance. For example, the gate oxide breakdown that continuously happens inside the MOSFET can cause its conduction resistance to increase. As a result, the ESS efficiency can be further reduced. If there is no proper maintenance or monitoring system, the ageing of switches may lead to their failure. This is more serious in the ESS since modules/cells may be short-circuited or even catch fire if the switches fail. Third, active balancing during the discharging process is discussed in this paper, while the charging process is not analysed. Theoretically, the proposed active balancing algorithms are also applicable during the charging process. Lithium-ion battery modules with a higher SOC tend to be in parallel connection, reducing the charging currents passing through them. However, the charging speed is another important factor. Therefore, the balance between the charging efficiency and charging speed should be considered while designing optimal charging strategies. Based on the above discussion, some future work can be suggested. For example, losses caused by switches need to be considered in the active balancing algorithms. The period for which a certain ESS configuration needs to be maintained can be optimised to reduce the sum of conduction and switching losses. Additionally, switch failures can be avoided by designing some switch ageing monitors. Furthermore, besides the discharging process, the proposed active balancing algorithms can be further developed to also achieve a fast and highly efficient charging process.

Author Contributions

BJ – Research concept and design; Collection and/or assembly of data; Data analysis and interpretation; Writing the article; Final approval of the article. YL –Critical revision of the article; Final approval of the article.

References

Biľanský, J. and Lacko, M. (2020). Design and Simulation of Cyclic Battery Tester. *Power Electronics and Drives*, 5(40), pp. 229–241, doi: 10.2478/pead-2020-0017.

Burke, A., Liu, Z. and Zhao, H. (2014). Present and Future Applications of Supercapacitors in Electric and Hybrid Vehicles. *2014 IEEE International Electric Vehicle Conference (IEVC)*, pp. 1–8, doi: 10.1109/IEVC.2014.7056094.

Caspar, M., Eiler, T. and Hohmann, S. (2018). Systematic Comparison of Active Balancing: A Model-Based Quantitative Analysis. In *IEEE Transactions on Vehicular Technology*, 67(2), pp. 920–934, doi: 10.1109/TVT.2016.2633499.

Chen, H., Xiong, R., Lin, C. and Shen, W. (2021). Model Predictive Control Based Real-Time Energy Management for Hybrid Energy Storage System. In *CSEE Journal of Power and Energy Systems*, 7(4), pp. 862–874, doi: 10.17775/CSEEJPES.2020.02180.

Ci, S., Lin, N. and Wu, D. (2016). Reconfigurable Battery Techniques and Systems: A Survey. In *IEEE Access*, 4, pp. 1175–1189, doi: 10.1109/ACCESS.2016.2545338.

East, S. and Cannon, M. (2020). Optimal Power Allocation in Battery/Supercapacitor Electric Vehicles Using Convex Optimization. In *IEEE Transactions on Vehicular Technology*, 69(11), pp. 12751–12762, doi: 10.1109/TVT.2020.3023186.

Frieske, B., Kloetzke, M. and Mauser, F. (2013). Trends in Vehicle Concept and Key Technology Development for Hybrid and Battery Electric Vehicles. *2013 World Electric Vehicle Symposium and Exhibition (EVS27)*, pp. 1–12, doi: 10.1109/EVS.2013.6914783.

Gunlu, G. (2017). Dynamically Reconfigurable Independent Cellular Switching Circuits for Managing Battery Modules. In *IEEE Transactions on Energy Conversion*, 32(1), pp. 194–201, doi: 10.1109/TEC.2016.2616190.

Han, W. and Kersten, A. (2020). Analysis and Estimation of the Maximum Circulating Current during the Parallel Operation of Reconfigurable Battery Systems. *2020 IEEE Transportation Electrification Conference & Expo (ITEC)*, pp. 229–234, doi: 10.1109/ITEC48692.2020.9161478.

Huang, W. and Abu Qahouq, J. A. (2015). Energy Sharing Control Scheme for State-of-Charge Balancing of Distributed Battery Energy Storage System. In *IEEE Transactions on Industrial Electronics*, 62(5), pp. 2764–2776, doi: 10.1109/TIE.2014.2363817.

Huang, X., Jiang, B. and Liu, Y. (2021). A Reconfigurable Battery Supercapacitor Hybrid Energy System with Active Balancing for Vehicle Applications. *2021 IEEE 19th International Power Electronics and Motion Control Conference (PEMC)*, pp. 231–236, doi: 10.1109/PEMC48073.2021.9432499.

Jiang, B., Liu, Y., Huang, X. and Prakash, R. R. R. (2020). A New Battery Active Balancing Method with Supercapacitor Considering Regeneration Process. *IECON 2020 The 46th Annual Conference of the IEEE Industrial Electronics Society*, pp. 2364–2369, doi: 10.1109/IECON43393.2020.9254839.

Khaligh, A. and Li, Z. (2010). Battery, Ultracapacitor, Fuel Cell, and Hybrid Energy Storage Systems for Electric, Hybrid Electric, Fuel Cell, and Plug-In Hybrid Electric Vehicles: State of the Art. In *IEEE Transactions on Vehicular Technology*, 59(6), pp. 2806–2814, doi: 10.1109/TVT.2010.2047877.

Kim, H. and Shin, K. G. (2009). On Dynamic Reconfiguration of a Large-Scale Battery System. *2009 15th IEEE Real-Time and Embedded Technology and Applications Symposium*, pp. 87–96, doi: 10.1109/RTAS.2009.13.

Kim, T., Qiao, W. and Qu, L. (2012). Power Electronics-Enabled Self-X Multicell Batteries: A Design Toward Smart Batteries. In *IEEE Transactions on Power Electronics*, 27(11), pp. 4723–4733, doi: 10.1109/TPEL.2012.2183618.

Kollmeyer, P., Wootton, M., Reimers, J., Stiene, T., Chemali, E., Wood, M. and Emadi, A. (2017). Optimal Performance of a Full Scale Li-ion Battery and Li-ion Capacitor Hybrid Energy Storage System for a Plug-in Hybrid Vehicle. *2017 IEEE Energy Conversion Congress and Exposition (ECCE)*, pp. 572–577, doi: 10.1109/ECCE.2017.8095834.

Kremzow-Tennie, S., Scholz, T., Friedbert, P., Alexander, P., Heiko, F. and Benedikt, S. (2022). A Comprehensive Overview of the Impacting Factors on a Lithium-Ion-Battery's Overall Efficiency. *Power Electronics and Drives*. 7(42), pp. 9-28, doi: 10.2478/pead-2022-0002

Lee, S., Noh, G. and Ha, J. I. (2021). Efficient and Reconfigurable Multi-cell Battery Pack for Portable Electronic Devices with Simultaneous Charging and Discharging Capability. *2021 IEEE 12th Energy Conversion Congress & Exposition - Asia (ECCE-Asia)*, pp. 1021–1026, doi: 10.1109/ECCE-Asia49820.2021.9479094.

Momayyezan, M., Hredzak, B. and Agelidis, V. G. (2016). Integrated Reconfigurable Converter Topology for High-Voltage Battery Systems. In

IEEE Transactions on Power Electronics, 31(3), pp. 1968–1979, doi: 10.1109/TPEL.2015.2440441.

Morstyn, T., Momayyezan, M., Hredzak, B. and Agelidis, V. G. (2016). Distributed Control for State-of-Charge Balancing Between the Modules of a Reconfigurable Battery Energy Storage System. In *IEEE Transactions on Power Electronics*, 31(11), pp. 7986–7995, doi: 10.1109/TPEL.2015.2513777.

Muhammad, S., Rafique, M. U., Li, S., Shao, Z., Wang, Q. and Liu, X. (2019). Reconfigurable Battery Systems: A Survey on Hardware Architecture and Research Challenges. *ACM Transactions on Design Automation of Electronic Systems*, 24, pp. 1–27, doi: 10.1145/3301301.

Omariba, Z. B., Zhang, L. and Sun, D. (2019). Review of Battery Cell Balancing Methodologies for Optimizing Battery Pack Performance in Electric Vehicles. In *IEEE Access*, 7, pp. 129335–129352, doi: 10.1109/ACCESS.2019.2940090.

Peprah, G. K., Liberati, F., Altaf, F., Osei-Dadzie, G., Di Giorgio, A. and Pietrabissa, A. (2021). Optimal Load Sharing in Reconfigurable Battery Systems using an Improved Model Predictive Control Method. *2021 29th Mediterranean Conference on Control and Automation (MED)*, pp. 979–984, doi: 10.1109/MED51440.2021.9480237.

Pinter, Z. M., Papageorgiou, D., Rohde, G., Marinelli, M. and Træholt, C. (2021). Review of Control Algorithms for Reconfigurable Battery Systems with an Industrial Example. *2021 56th International Universities Power Engineering Conference (UPEC)*, pp. 1–6, doi: 10.1109/UPEC50034.2021.9548259.

Piriienko, S., Beshta, A., Balakhontsev, A., Khudoliy, S. and Albu, A. (2016). Optimization of Hybrid Energy Storage System for Electric Vehicles. *Power Electronics and Drives*, 1(36)(2), pp. 97–111, doi:10.5277/PED160206.

Salari, O., Zaad, K. H., Bakhshai, A. and Jain, P. (2020). Reconfigurable Hybrid Energy Storage System for an Electric Vehicle DC–AC Inverter. In *IEEE Transactions on Power Electronics*, 35(12), pp.12846–12860,doi:10.1109/TPEL.2020.2993783.

Schmid, M., Gebauer, E. and Endisch, C. (2021). Structural Analysis in Reconfigurable Battery Systems for Active Fault Diagnosis. In *IEEE Transactions on Power Electronics*, 36(8), pp. 8672–8684, doi: 10.1109/TPEL.2021.3049573.

Viswanathan, V., Palaniswamy, L. N. and Leelavinodhan, P. B. (2019). Optimization Techniques of Battery Packs Using Reconfigurability: A Review. *Journal of Energy Storage*, 23, pp. 404–415, doi: 10.1016/j.est.2019.03.002.

Xia, Z. and Abu Qahouq, J. A. (2021). State-of-Charge Balancing of Lithium-Ion Batteries With State-of-Health Awareness Capability. In *IEEE Transactions on Industry Applications*, 57(1), pp. 673–684, doi: 10.1109/TIA.2020.3029755.

Ye, Y., Cheng, K. W. E., Fong, Y. C., Xue, X. and Lin, J. (2017). Topology, Modeling, and Design of Switched-Capacitor-Based Cell Balancing Systems and Their Balancing Exploration. In *IEEE Transactions on Power Electronics*, 32(6), pp. 4444–4454, doi: 10.1109/TPEL.2016.2584925.

Zhou, S., Chen, Z., Huang, D. and Lin, T. (2021). Model Prediction and Rule Based Energy Management Strategy for a Plug-in Hybrid Electric Vehicle With Hybrid Energy Storage System. In *IEEE Transactions on Power Electronics*, 36(5), pp. 5926–5940, doi: 10.1109/TPEL.2020.3028154.